Case Studies in Construction Materials 19 (2023) e02444

Contents lists available at ScienceDirect

Case Studies in Construction Materials

journal homepage: www.elsevier.com/locate/cscm

Application of waste ceramic powder as a cement replacement in reinforced concrete beams toward sustainable usage in construction

Ceyhun Aksoylu [a], Yasin Onuralp Özkılıç [b,*], Alireza Bahrami [c,*], Sadık Alper Yıldızel [d], Ibrahim Y. Hakeem [e], Nebi Özdöner [b], Boğaçhan Başaran [f], Memduh Karalar [g]

[a] Department of Civil Engineering, Faculty of Engineering and Natural Sciences, Konya Technical University, Konya 42250, Turkey
[b] Department of Civil Engineering, Faculty of Engineering, Necmettin Erbakan University, Konya 42000, Turkey
[c] Department of Building Engineering, Energy Systems and Sustainability Science, Faculty of Engineering and Sustainable Development, University of Gävle, 801 76 Gävle, Sweden
[d] Civil Engineering Department, Faculty of Engineering, Karamanoglu Mehmetbey University, Karaman, Turkey
[e] Department of Civil Engineering, College of Engineering, Najran University, Najran, Saudi Arabia
[f] Department of Construction, Vocational School of Technical Sciences, Amasya University, Amasya 05100, Turkey
[g] Department of Civil Engineering, Faculty of Engineering, Zonguldak Bulent Ecevit University, Zonguldak, Turkey

ARTICLE INFO

Keywords:
Ceramic powder
Concrete
Beam
Flexural strength
Waste
Recycled
Sustainability

ABSTRACT

The main purpose of this study was to investigate the flexural behavior of reinforced concrete beams (RCBs) containing waste ceramic powder (CP) as partial replacement of cement. For this purpose, flexural tests were carried out using various amounts of mixing ratios. By determining the amount of CP utilized in the optimum ratios, it was aimed both to make predictions for design engineers and to show its beneficial effect on the environment by recycling the waste material. For this purpose, twelve specimens were produced and verified to monitor the flexural behavior. The longitudinal reinforcements percentage (0.77%, 1.21%, and 1.74%) and CP percentage (0%, 10%, 20%, and 30%) were chosen as the parameters. CP could be effectively used up to 10% of cement as a replacement material. Increasing the CP percentage by more than 10% could considerably reduce the load-carrying capacity, ductility, and stiffness of RCBs, specifically when the longitudinal reinforcements percentage was high. In other words, as CP increased from 0% to 30%, the load-carrying capacity decreased between 0.4% and 27.5% compared with RCBs with the longitudinal tension reinforcements of 2ϕ8 without CP. However, reductions of 5.5–39.8% and 2.15–39.5% in the load-carrying capacity occurred respectively compared with RCBs with the longitudinal tension reinforcements of 2ϕ10 and 2ϕ12 without CP. The achieved longitudinal reinforcements percentage was close to the balanced ratio, while more than 10% CP cannot be used without any precautions for mixtures.

* Corresponding authors.
E-mail addresses: yozkilic@erbakan.edu.tr (Y.O. Özkılıç), alireza.bahrami@hig.se (A. Bahrami).

https://doi.org/10.1016/j.cscm.2023.e02444
Received 13 April 2023; Received in revised form 2 August 2023; Accepted 30 August 2023
Available online 1 September 2023

1. Introduction

In recent years, durable, renewable, and sustainable materials have become famous to researchers in order to have cleaner and greener construction in the construction industry [1–4,78]. Especially in the literature, various research works have been carried out on the mechanical properties and flexural and shear strengths of these renewable and sustainable materials [5–17]. Among them, concrete is the most commonly used artificial material, and new advances are always encouraged [18–21,79]. An annual natural consumption of concrete has reached up to 15 billion tons [22,23], since it is used in many different applications [80–82]. The reuse of waste materials can benefit the environment by lowering the consumption of nonrenewable natural resources and reducing landfill problems [24–28]. The effective utilization of natural resources and the minimization of industrial wastes are among the main strategies of greener production [29–31]. From the construction sector's perspective, the use of recycled industrial waste is of great importance to protect natural resources [32,33].

In addition, ceramic is generally preferred in the production of composite materials. The utilization of waste ceramic is undoubtedly vital for a greener global production and waste-based construction industry. Zimbili et al. [34] stated that ceramic has the highest usage rate of 54% among all construction waste materials. The consumption of locally existing ceramic waste as a replacement for the concrete ingredients might resolve the vital environmental problem [35] as the limited usage of cement and aggregates in areas where they are rare and costly [36]. On the other hand, the global manufacture of tiles demonstrates a progression of about 5.2%, with 13.5 million m^2 in 2018 from 8.6 million m^2 in 2008 [37]. For these reasons, this topic constitutes a growing and popular research direction for researchers in the industry. Nowadays, many researchers work on recycled concrete and recycled ceramic powder (CP) concrete.

Various studies in the literature indicate that ceramic materials have a strong resistance to biodegradation forces [38–41]. Due to its high crystalline aluminum and silica properties, ceramic is considered a valuable material as an auxiliary cement to increase the strength and durability of binding materials and ceramic incorporated concrete [42–44]. Mukai et al. [45] utilized recycled concrete for structural applications. They designed reinforced concrete beams (RCBs) with the cross-sectional dimension of 15 × 15 cm with the length of 180 cm by using reprocessed aggregates at the ratios of 15% and 30% replacement levels. The study's results illustrated an unimportant variance in the ultimate flexural capacity of RCBs with the waste aggregates compared with the reference specimen. Mukai and Kikuchi [46] performed several tests on RCBs having 15% and 30% recycled concrete aggregate replacements and described that there was no critical change in the ultimate moment with a minor cracking moment for RCBs. Pacheco-Torgal and Jalali [47] examined the possibility of using ceramic wastes in concrete production. They found that concrete with 20% cement replacement had an insignificant strength loss and increased the durability properties. Furthermore, in the same study, it was found that concrete designs with incorporated ceramic aggregates (up to 20% replacement ratio) reflected better results concerning the strength and durability properties, leading to more durable concrete structures. Ikponmwosa and Ehikhuenmen [48] investigated the flexural performance of unreinforced beams and RCBs in terms of the ceramic waste addition as the aggregate replacement material. They tested 45 unreinforced beams (150 × 150 × 750 mm) and RCBs (150 × 250 × 2150 mm) to evaluate their flexural strengths. It was discovered that increasing the ceramic waste content resulted in a noticeable reduction in the failure load, leading to higher experimental moments compared with theoretical moments. Another experimental study was conducted by Fatima et al. [49] on the same topic. They observed the possibility of consuming ceramic dust with a particle size less than 75 μm for the partial replacement of cement in concrete production. They did various mechanical tests including the determination of the compressive strength, modulus of elasticity, splitting tensile strength, and flexural strength. It was found that the flexural strength reduced with increasing the ceramic waste contents. It was also witnessed that the flexural strength reduction declined after a 10% addition of ceramic waste. Samadi et al. [22] assessed the flexural tests results of five RCBs (160 × 200 × 2200 mm) produced with reused ceramic as the aggregate and cement

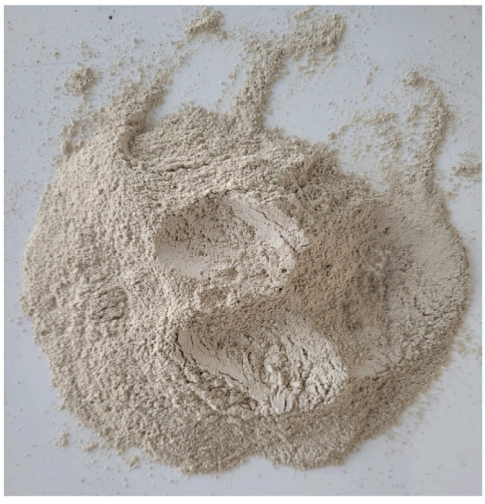

Fig. 1. CP.

replacement materials to compare the experimental results with the unreinforced control specimen. They found that in all the reused ceramic aggregate utilizations, the properties of the beams such as the yield and ultimate loads displayed a similar trend. In addition, it was stated that ceramic waste could be employed in every part of the high-performance concrete in accordance with the structural requirements.

As can be realized from the earlier studies in the literature, several research works were attempted on the performance of waste materials incorporated in concrete [38,50,51]. Researchers have recognized variations in the properties of concrete, but they have limited discussions on the effects of the CP utilization as a cement replacement material on the structural behavior of RCBs. This research work was carried out in order to expand the limited knowledge in this field and to contribute to new studies. Unlike studies in the literature, the bending performance of RCBs was investigated by determining the optimum CP ratio. Thus, this article concentrated on the utilization and influences of CP on the flexural performance of RCBs with different longitudinal reinforcements ratios.

2. Material and methods

In order to cast the sustainable concrete, CEM I 32.5 cement was used with specific percentages of fine aggregate (FA) and coarse aggregate (CA) combined with waste CP to examine the strength properties. CP is presented in Fig. 1. The purpose of the recycled concrete mixtures was to obtain the optimal combination in terms of adequate performance requirements. To achieve to this goal, waste CP was utilized with the replacement ratios of 10%, 20%, and 30% by the weight of cement. The material properties of cement, aggregates, and CP are listed in Table 1. The mixture designs of the beams are given in Table 2.

The mixture designs were considered for the compression and splitting tensile tests. The compressive strength of concrete with CP was determined by taking three cube specimens of 150 × 150 × 150 mm. The average compressive strengths of 19.3 MPa, 18.2 MPa, 15.1 MPa, and 10.2 MPa were obtained for concrete with 0%, 10%, 20%, and 30% waste CP, respectively. Moreover, the splitting tensile tests were done by taking three cylindrical specimens of 100 × 200 mm. The mean splitting tensile strengths were achieved as 1.55 MPa, 1.45 MPa, 1.37 MPa, and 1 MPa with 0%, 10%, 20%, and 30% waste CP, respectively. The results of the strengths tests are depicted in Fig. 2.

Half-scale RCBs with CP blended concrete were poured into the molds. Two variables were considered for the experimental tests of RCBs including the ratio of waste CP and the ratio of longitudinal reinforcements. Moreover, three specimens were casted to obtain the reference specimens without CP. All the specimens had a length of 1000 mm and cross-section of 100 × 150 mm. The stirrups were employed as ϕ6 at 100 mm spaces to obtain the flexural behavior. The typical reinforcements detail of RCBs is shown in Fig. 3.

The longitudinal tension reinforcements of 2ϕ12, 2ϕ10, and 2ϕ6 were used. The test setup consisting of a servo-controlled hydraulic is illustrated in Fig. 4. Moreover, the details of the test specimens are presented in Table 3.

3. Theoretical calculations

3.1. Calculation of flexural strengths of RCBs

A numerical method and the equivalent rectangular stress distribution method were utilized to calculate the flexural strengths of RCBs. In the numerical method, a computer program was written to calculate the carrying capacity of the beam sections, Eq. 5, by using suitability (Eqs. 1–2) and equilibrium equations (Eqs. 3–4) for evaluating the beam sections' carrying capacity. The program was developed employing Microsoft Excel and Visual Basic for Applications (VBA) software.

Table 1
Material properties of cement, aggregates, and CP.

Parameter	Percentage (by mass)/Value	
CEM I 32.5		**CP**
SiO_2	20.34	65.94
Al_2O_3	5.3	21.74
CaO	63.01	2.43
Na_2O	—	1.45
K_2O	—	2.74
ZrO_2	—	1.52
SO_3	2.6	—
Cl	0.01	—
Free CaO	0.79	—
MgO	1.72	—
Fe_2O_3	2.69	1.39
LoI	1.71	—
Specific surface (m^2/g)	0.3864	—
Compressive strength at 28 days (MPa)	43.11	—
Volumetric stability (mm)	< 9.5	—
FA		**CA**
Specific gravity (SSD)	2.63	2.59
Water absorption	2.23	0.74
Fineness modulus	1.64	7.39

Table 2
Mixture designs of RCBs.

Mixture	Cement (kg/m^3)	Water (kg/m^3)	FA (kg/m^3)	CA (kg/m^3)	CP (kg/m^3)
0%	580	270	785	900	0
10%	522				58
20%	464				116
30%	406				174

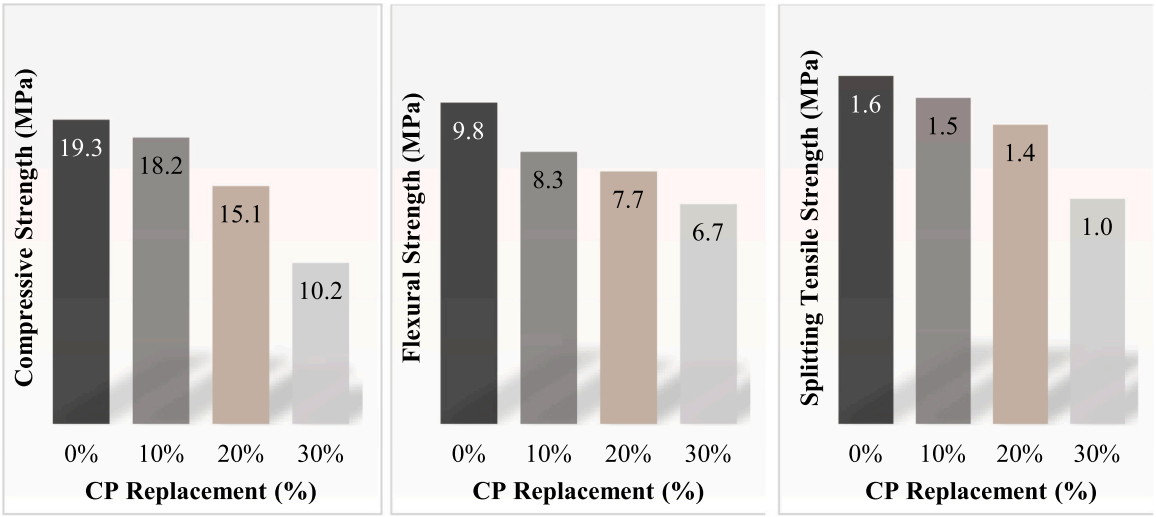

Fig. 2. Results of experimental tests.

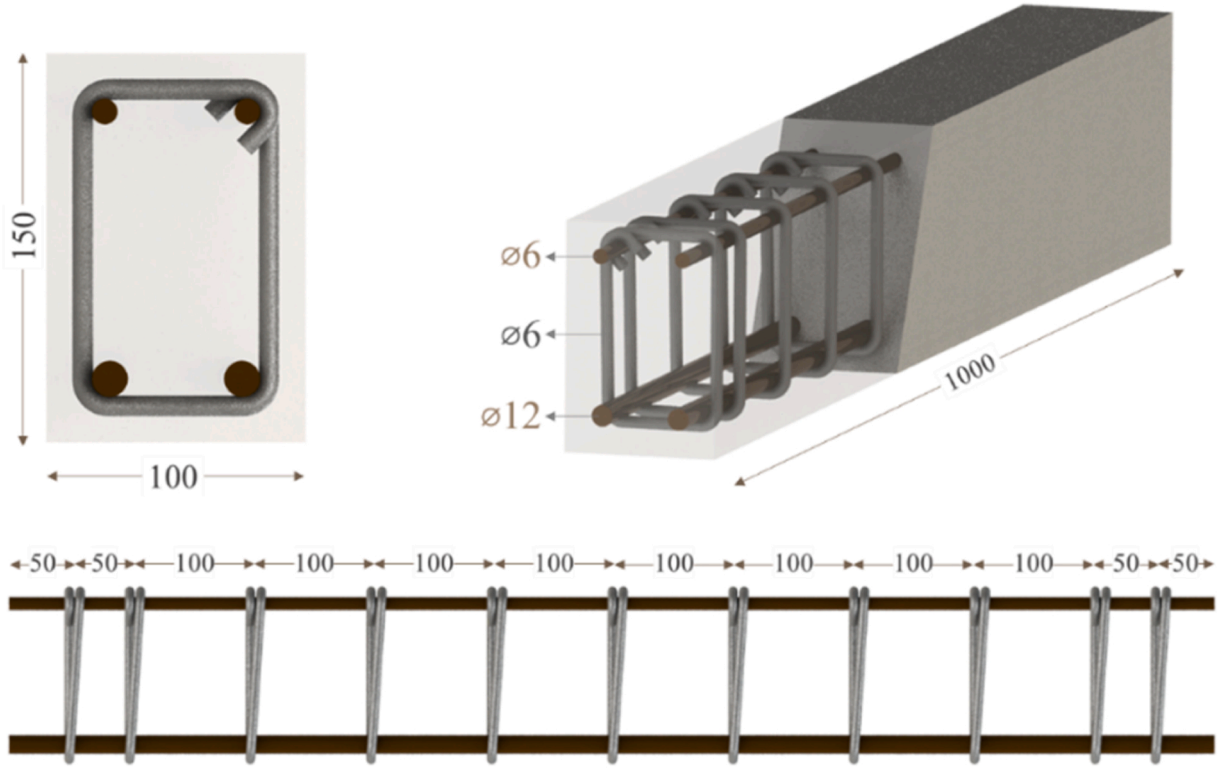

Fig. 3. Reinforcements detail of RCBs (units are mm).

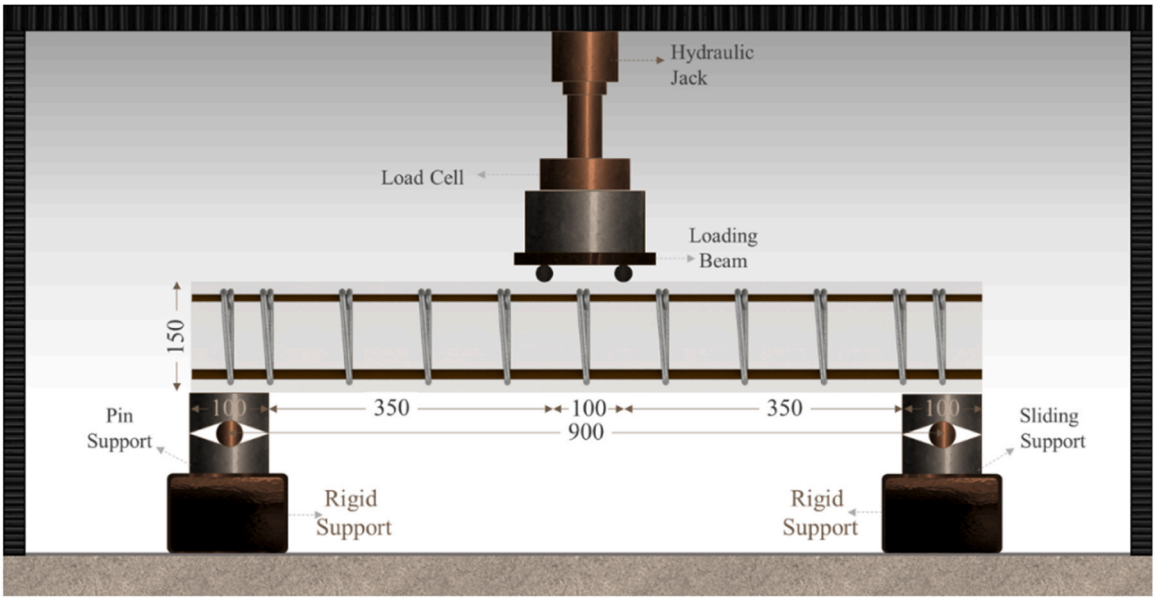

Fig. 4. Test setup (units are mm).

Table 3
Details of test specimens.

No.	Name of Test Specimen	Compression Reinforcement	Tension Reinforcement	Tension Reinforcement Ratio	Waste CP
1	B8–0	2ϕ6	2ϕ8	0.0077	0%
2	B8–10	2ϕ6	2ϕ8	0.0077	10%
3	B8–20	2ϕ6	2ϕ8	0.0077	20%
4	B8–30	2ϕ6	2ϕ8	0.0077	30%
5	B10–0	2ϕ6	2ϕ10	0.0121	0%
6	B10–10	2ϕ6	2ϕ10	0.0121	10%
7	B10–20	2ϕ6	2ϕ10	0.0121	20%
8	B10–30	2ϕ6	2ϕ10	0.0121	30%
9	B12–0	2ϕ6	2ϕ12	0.0174	0%
10	B12–10	2ϕ6	2ϕ12	0.0174	10%
11	B12–20	2ϕ6	2ϕ12	0.0174	20%
12	B12–30	2ϕ6	2ϕ12	0.0174	30%

In the program, depending on the increase in the deformation in the top compression fiber in the compression region of the beam, other unknowns were calculated iteratively until the equilibrium equations and compliance conditions were met (Fig. 5).

$$c_i = \frac{\varepsilon_{ci} d}{\varepsilon_{ci} + \varepsilon_{si}} \tag{1}$$

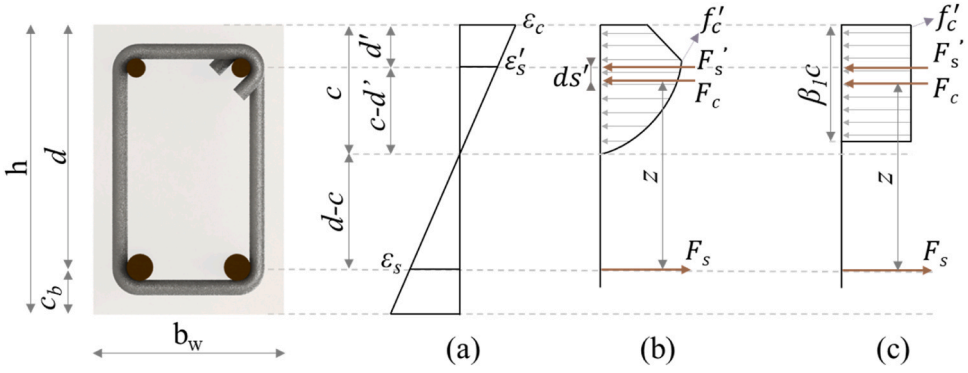

Fig. 5. In beam section: (a) strain diagram, (b) theoretical stress diagram, and (c) equivalent stress block diagram.

$$c_i = \frac{\varepsilon_{ci} d'}{\varepsilon_{ci} - \varepsilon_{si}'} \tag{2}$$

$$F_{si} = F_{ci} + F_{si}' \tag{3}$$

$$c_i = \frac{A_s f_{si} - A_s' f_{si}'}{f_{ci}' b_w k_i} \tag{4}$$

$$M_{ni} = A_s f_{si} z_i + A_s' f_{si}' d_{si}' \tag{5}$$

Here, c_i is the depth of the concrete compression block (mm), d is the effective height (mm), d' is the distance from the top of the beam to the center of the compression reinforcements (mm), ε_{ci} is the unit strain of the outermost fiber of the concrete compression block, ε_{si} is the unit strain of the tension reinforcements, ε_{si}' is the unit strain of the compression reinforcements, ε_{cti} is the concrete unit strain of outermost fiber of tension block, A_s is the tension reinforcements area (mm^2), A_s' is the compression reinforcements area (mm^2), b_w is the beam width (mm^2), k_i is the equivalent stress block depth coefficient, f_{si} is the stress of the tension reinforcements (MPa), f_{si}' is the stress of the compression reinforcements (MPa), f_{ci} is the compressive stress of concrete (MPa), F_{si} is the force of the tension reinforcements (N), F_{si}' is the force of the compression reinforcements (N), F_{ci} is the compressive force of concrete (N), M_{ni} is the moment-carrying capacity of the section (Nmm), z_i is the distance between the center of gravity of the concrete compression block and the center of gravity of the tension reinforcements (mm), d_{si}' is the distance between the outermost fiber of the concrete compression block and the center of gravity of the compression reinforcements (mm), and the index i in the terms is the number of steps of the iteration.

Three different concrete stress-strain models were proposed by Hognestad [52], Park et al. [53], and Todeschini et al. [54]. These models have been used separately in the numerical analysis to calculate the beams' carrying capacity. In addition, the stress-strain curve of steel has been considered as an idealized trilinear model (Fig. 6).

Hognestad's proposed concrete stress-strain relationship [52] is provided in Eq. 6-10. In the equations, f_c' is the cylinder compressive strength of concrete, E_c is the modulus of elasticity of concrete, ε_{co} is the unit strain of concrete under maximum force, f_{ci} is the compressive stress of concrete corresponding to the ith step strain of concrete, and ε_{cu} is the final unit strain of concrete.

$$f_c'' = 0.85 f_c' \tag{6}$$

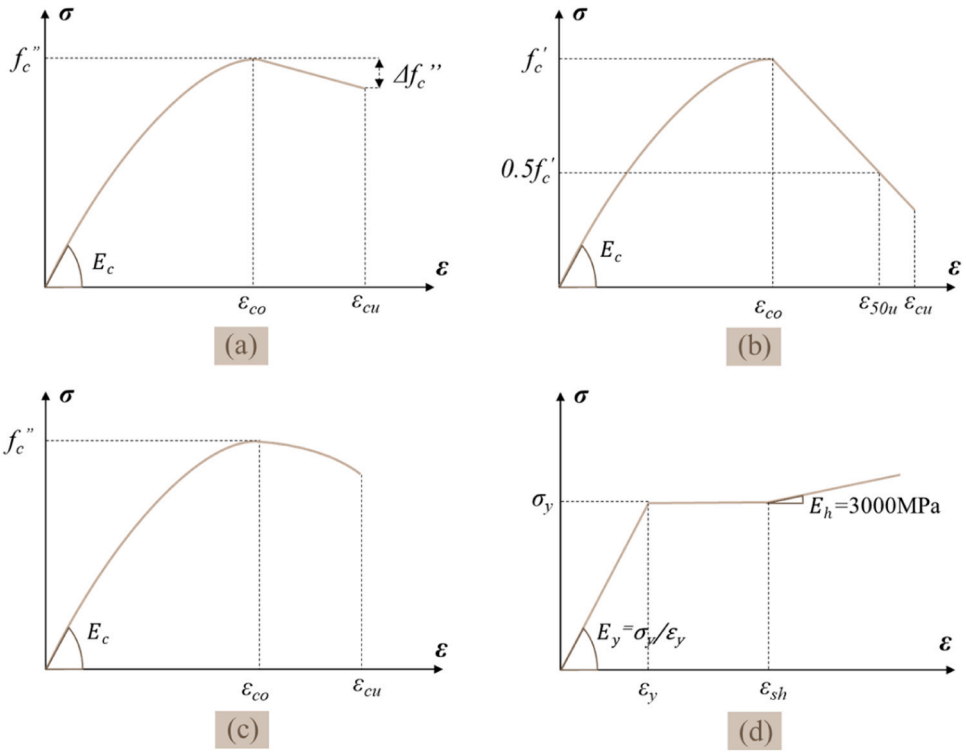

Fig. 6. Stress-strain models: (a) stress-strain model of concrete by Hognestad [52], (b) stress-strain model of concrete by Park et al. [53], (c) stress-strain model of concrete by Todeschini et al. [54], and (d) stress-strain model of tension steel reinforcements.

$$E_c = 12680 + 460 f_c^{'} \tag{7}$$

$$\varepsilon_{co} = \frac{2 f_c^{'}}{E_c} \tag{8}$$

$$f_{ci} = f_c^{'}\left[2\frac{\varepsilon_{ci}}{\varepsilon_{co}} - \left(\frac{\varepsilon_{ci}}{\varepsilon_{co}}\right)^2\right] \qquad \varepsilon_{ci} \le \varepsilon_{co} \tag{9}$$

$$f_{ci} = f_c^{'}\left[1 - 0.15\left(\frac{\varepsilon_{ci} - \varepsilon_{co}}{\varepsilon_{cu} - \varepsilon_{co}}\right)\right] \qquad \varepsilon_{co} < \varepsilon_{ci} \le \varepsilon_{cu} = 0.0038 \tag{10}$$

The stress-strain relationship of the developed model proposed by Park et al. [53] is given in Eqs. 11–14. In the equations, $\varepsilon_{cu} = 0.004$ was considered. Eq. 15, recommended in ACI 318–19 [55], was utilized to determine the modulus of elasticity of concrete in the carrying capacity calculations using these equations.

$$f_{ci} = f_c^{'}\left[2\frac{\varepsilon_{ci}}{\varepsilon_{co}} - \left(\frac{\varepsilon_{ci}}{\varepsilon_{co}}\right)^2\right] \qquad \varepsilon_{ci} \le \varepsilon_{co} = 0.002 \tag{11}$$

$$f_{ci} = f_c^{'}[1 - Z_u(\varepsilon_{ci} - \varepsilon_{co})] \qquad \varepsilon_{co} < \varepsilon_{ci} \le \varepsilon_{cu} = 0.004 \tag{12}$$

$$Z_u = \frac{0.5}{\varepsilon_{50u} - \varepsilon_{co}} \tag{13}$$

$$\varepsilon_{50u} = \frac{3 + 0.29 f_c^{'}}{145 f_c^{'} - 1000} \qquad \varepsilon_{co} \le \varepsilon_{50u} \tag{14}$$

$$E_c = 4700\sqrt{f_c^{'}} \tag{15}$$

The stress-strain relationship of concrete proposed by Todeschini et al. [54] is presented in Eq. 16-18. In the equations, $\varepsilon_{cu} = 0.0038$ was taken.

$$f_c^{'} = 0.9 f_c^{'} \tag{16}$$

$$\varepsilon_{co} = \frac{1.71 f_c^{'}}{E_c} \tag{17}$$

$$f_{ci} = \frac{2 f_c^{'}\left(\frac{\varepsilon_{ci}}{\varepsilon_{co}}\right)}{1 + \left(\frac{\varepsilon_{ci}}{\varepsilon_{co}}\right)^2} \qquad \varepsilon_{ci} \le \varepsilon_{cu} = 0.0038 \tag{18}$$

The stress-strain relationship of the steel reinforcements is indicated in Eqs. 19–21. Here, f_y is the yield stress of the steel reinforcements, E_y is the modulus of elasticity of the steel reinforcements, E_{sh} is the hardening elastic modulus of the steel reinforcements, and ε_{sh} is the unit strain at the time that the steel reinforcements begin to harden. The current study considered the hardening modulus of elasticity as 3000 MPa.

$$f_{si} = E_y \varepsilon_{si} \qquad \varepsilon_{si} \le \varepsilon_y \tag{19}$$

$$f_{si} = f_y \qquad \varepsilon_y < \varepsilon_{yi} \le \varepsilon_{sh} = 0.02 \tag{20}$$

$$f_{si} = f_y + E_{sh}(\varepsilon_{si} - \varepsilon_{sh}) \qquad \varepsilon_{sh} < \varepsilon_{yi} \tag{21}$$

In this study, the equivalent rectangular stress distribution method proposed in ACI 318–19 [55] was used as the second method to obtain the moment-carrying capacity of the section (Eqs. 22–23). In the equations, β_1 is the correction coefficient for the concrete compressive stress block.

$$\beta_1 c = \frac{A_s f_{si} + A_s^{'} f_{si}^{'}}{0.85 f_{ci}^{'} b_w} \tag{22}$$

$$M_n = A_s f_{si}\left(d - \frac{\beta_1 c}{2}\right) + A_s^{'} f_{si}^{'}\left(\frac{\beta_1 c}{2} - d^{'}\right) \tag{23}$$

3.2. Calculation of shear capacity of RCBs

ACI 318–19 [55] proposed a model in which the contribution of concrete to the shear capacity (V_c), Eq. 24, and the contribution of the stirrups to the shear capacity (V_s), Eq. 25, are considered together to determine the total shear capacity of RCBs. In this model, the RCBs' so-called total shear capacity (V_n) can be calculated by Eq. 26. In the equations, ρ_w is the tension reinforcements ratio, s is the stirrups spacing, f_{yt} is the yield stress of the stirrups, and A_w is the total area of the stirrup arms.

$$V_c = 0.66\sqrt[3]{\rho_w}\sqrt{f'_c}b_w d \le 0.42\lambda\sqrt{f'_c}b_w d \tag{24}$$

$$A_v \ge A_{v,\min} = 0.062\sqrt{f'_c}\,\frac{b_w}{f_{yt}}s$$

$$A_v \ge A_{v,\min} = 0.35\frac{b_w}{f_{yt}}s$$

$$V_s = \frac{A_w f_{yt}}{s}d \le 0.66\sqrt{f'_c}b_w d \tag{25}$$

$$V_n = V_c + V_s \tag{26}$$

4. Results and discussion

4.1. Failure modes and damage analysis

The failure modes of the specimens are demonstrated in Figs. 7, 8, and 9. In addition, crack patterns of the specimens are indicated in Fig. 10. The failure patterns of the tested RCBs with the tension reinforcements diameter of ϕ8 and the lowest tension reinforcements ratio (0.0077) are displayed in Fig. 7. In these RCBs, flexural cracks perpendicular to the beam axis were occurred due to the normal tensile stresses in the middle regions of B8–0 and B8–10 with 0% and 10% CP, respectively. By increasing the loads, vertical flexural cracks propagated toward the compression region of RCBs, while oblique cracks were formed in the shear opening of the beams owing to the principal tensile stresses. With further increase of the loads, the vertical cracks reached the compression zone of the beams, and these RCBs collapsed by reaching their flexural capacity. While similar behavior was observed in B8–20 with 20% CP, the transverse reinforcements reached their yield stress just before the tension reinforcements yielded in this beam. For this reason, oblique cracks developed faster than vertical flexural cracks and caused the beam to collapse before reaching its total capacity. In B8–30 with 30% CP, shear failure occurred due to the sudden development of the oblique cracks made by yielding of the transverse reinforcements before the tension reinforcements yielded.

The failure patterns of the tested RCBs with the tension reinforcements diameters of ϕ10 (ρ = 0.0121) and ϕ12 (ρ = 0.0174) are depicted in Figs. 8 and 9, respectively. Among these RCBs, reference B10–0 and 10% CP blended B10–10 showed similar behavior to B8–10 and B8–20, respectively. In B10–0, inclined cracks developed faster than vertical flexural cracks owing to the transverse

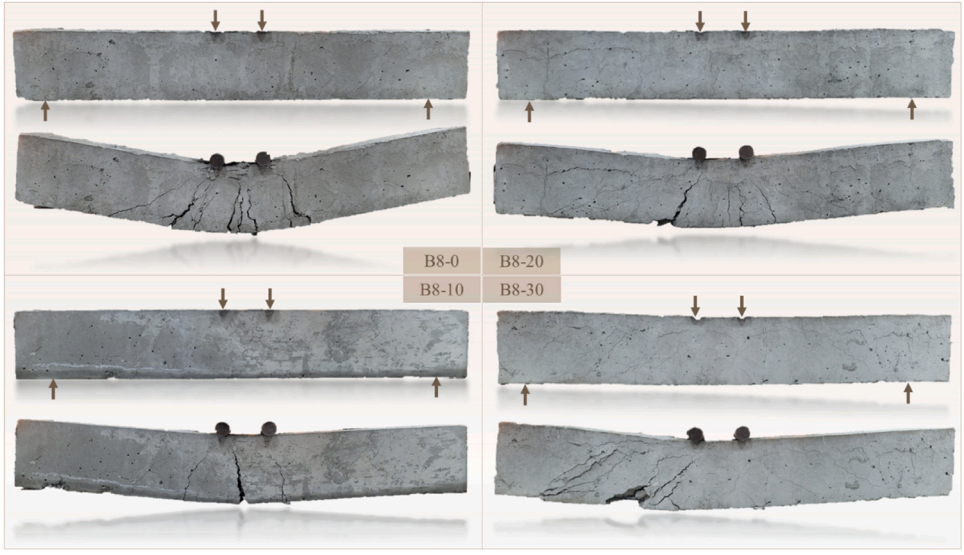

Fig. 7. Failure modes of RCBs with reinforcements ratio of 0.0077.

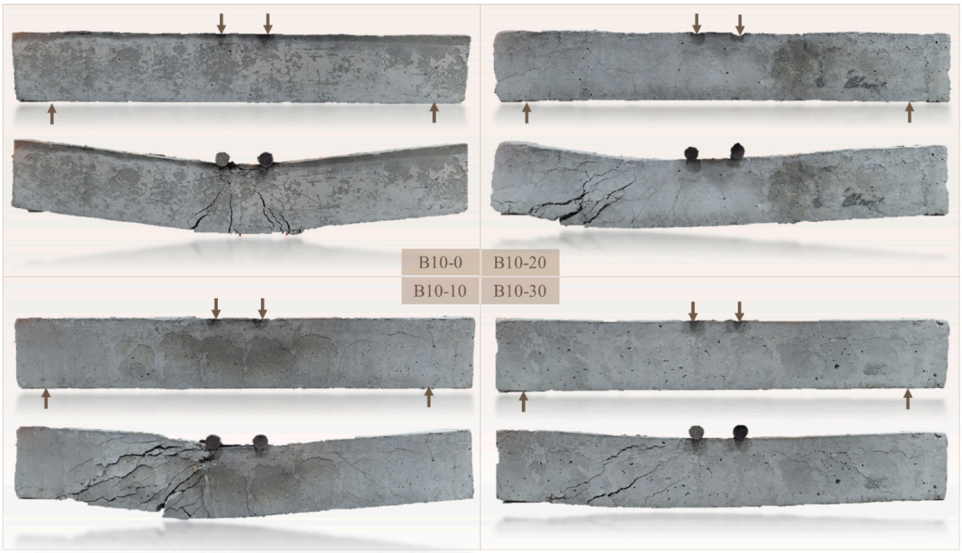

Fig. 8. Failure modes of RCBs with reinforcements ratio of 0.0121.

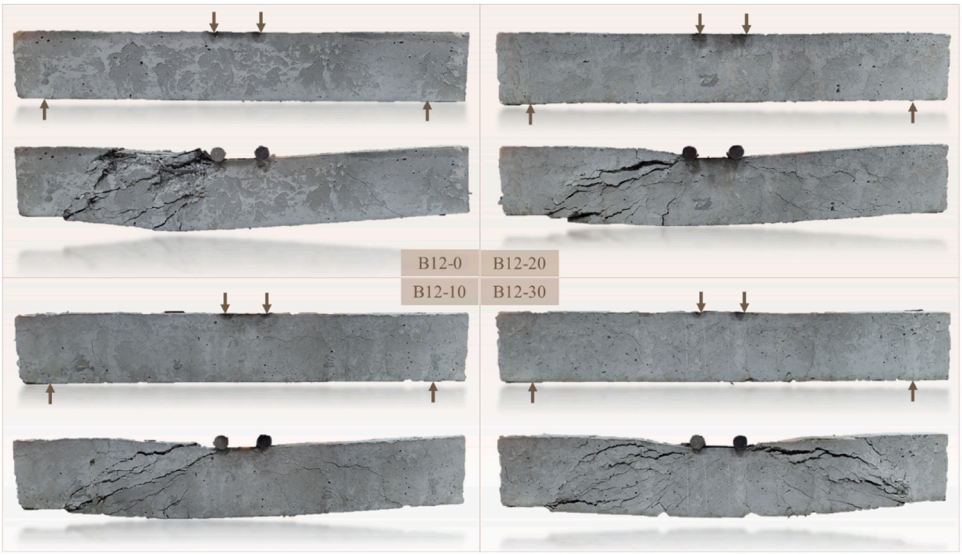

Fig. 9. Failure modes of RCBs with reinforcements ratio of 0.0174.

reinforcements reaching their yielding capacity after the tension reinforcements yielded, causing the beam to collapse before reaching total flexural capacity. In B10–10, on the other hand, just before the tension reinforcements yielded, the transverse reinforcements reached their yield stress, and the inclined cracks were formed together with the vertical flexural cracks, and the beam collapsed because of the propagation of the oblique cracks, however, not very suddenly. Because of this reason, the beam could not reach its total capacity. In all other RCBs (B10–20, B10–30, and B12 series), shear failure occurred due to the sudden development of the oblique cracks in the shear opening of the beams, owing to the principal tensile stresses before yielding of the tension reinforcements.

As the tension reinforcements ratio (ρ) in the tested RCBs increased from 0.0077 to 0.0174, the shear force demand from RCBs increased owing to the enhancing carrying capacities of RCBs. Further, as the CP content of RCBs increased from 0% to 30%, the shear capacity of RCBs decreased because of the decrease in the compressive strength of concrete. However, although the stirrup ratios in all RCBs were designed to prevent the shear failure, unexpected shear or flexural shear failure was observed in RCBs other than B8–0 and B8–10. It can also be noted that the flexural cracks turned into shear cracks with increasing the CP content resulting in the final collapses. Additionally, CP of more than 10% adversely affected all the specimens' carrying capacity. This situation can be attributed to the compressive strength decreasing effect by CP when it was utilized more than 15% by weight of cement leading to the reduction in the cement binder amounts [56,57]. In the earlier investigations, similar results were found. The decrease in the compressive strength

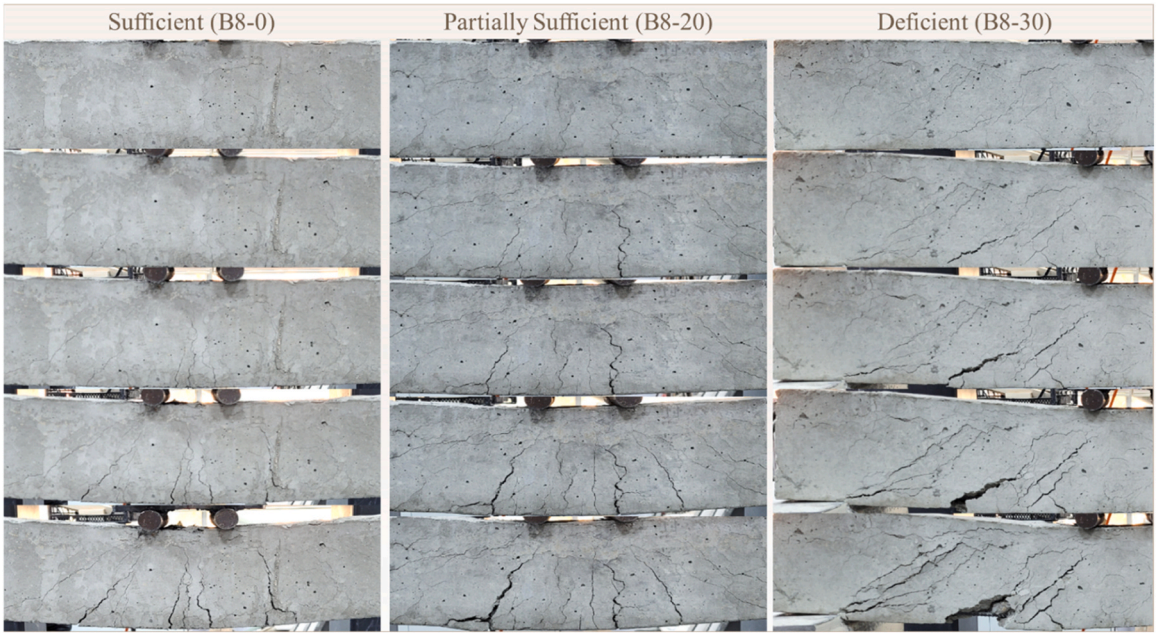

Fig. 10. Crack patterns of specimens.

was mainly the result of the immature pozzolanic reaction in concrete, and the preventive growth of C–S–H gel was affected as a result of the constituents in CP [39].

4.2. Load-displacement curves

The obtained load-displacement curves from the experimental tests on the twelve tested RCBs are illustrated in Figs. 11–13. Moreover, the achieved load and displacement values from the experimental tests are summarized in Table 4. Compared with the other specimens, B8–0 and B8–10 had the highest maximum displacement results, as expected, due to their reinforcements type, content, and low reinforcements ratio. As the reinforcements ratio increased, the specimen's carrying capacity enhanced while the ductility decreased. Displacements and rigidities at P_{max} and P_y are also given in Table 4. The CP inclusion of more than 10% significantly reduced the maximum and ultimate loads at similar intervals. Furthermore, it can be seen from Table 4 that P_{max} and P_y of B8–10 were least affected by the addition of 10% CP. In B8–10, the load-carrying capacity decreased by only 0.4%. This situation can be attributed to decreasing the tension reinforcements ratio compared with the other specimens [58,59]. Because as the tension reinforcements ratio in the beam decreases, the demanded shear force also decreases. In B10–10 and B12–10, 10% CP decreased the beams' load-carrying

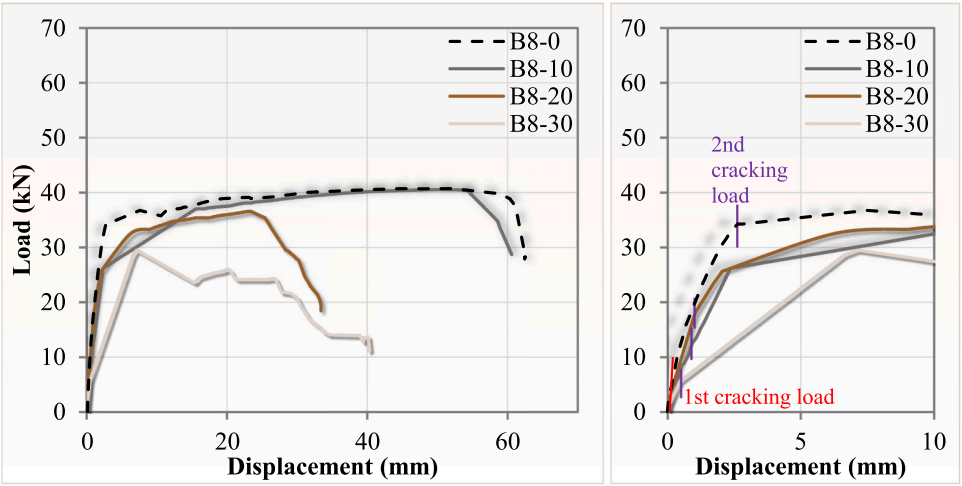

Fig. 11. Load-displacement (mid-span) relations of RCBs with reinforcements ratio of 0.0077.

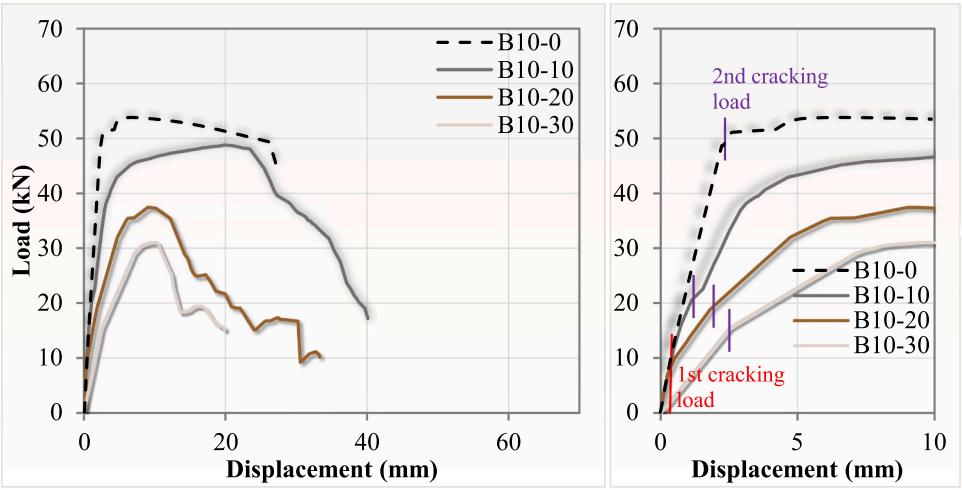

Fig. 12. Load-displacement (mid-span) relations of RCBs with reinforcements ratio of 0.0121.

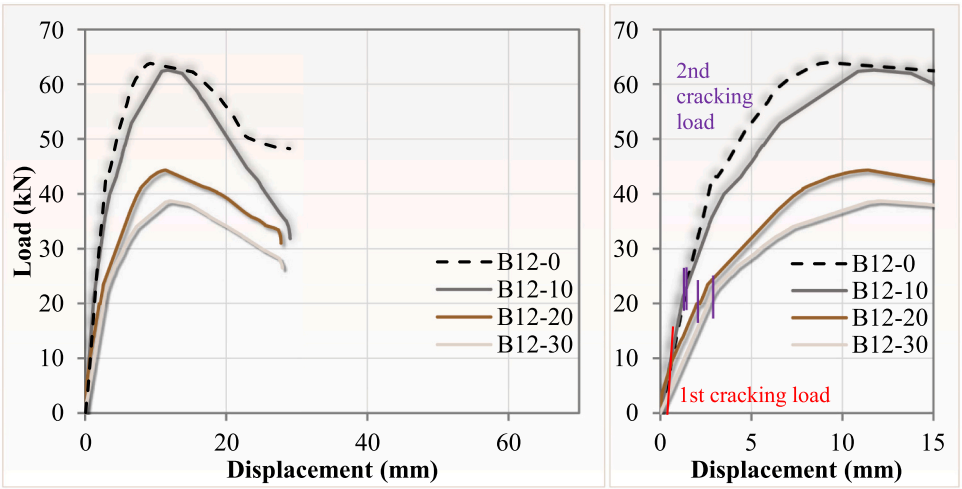

Fig. 13. Load-displacement (mid-span) relations of RCBs with reinforcements ratio of 0.0174.

Table 4
Obtained load and displacement values from experimental tests.

Test Specimen	P_{max} (kN)	δ_{Pmax} (mm)	S_{Pmax} (kN/mm)	P_y (kN)	δ_y (mm)	S_y (kN/mm)	δ_u (mm)	Ductility Ratio
B8–0	40.73	52.09	0.78	34.62	3.49	9.91	61.56	17.62
B8–10	40.55	50.49	0.80	34.47	12.45	2.77	58.67	4.71
B8–20	36.60	23.36	1.57	31.11	5.38	5.78	27.56	5.12
B8–30	29.52	7.14	4.14	25.09	5.68	4.42	16.56	2.92
B10–0	51.65	4.21	12.28	43.91	2.01	21.81	27.11	13.47
B10–10	48.80	19.85	2.46	41.48	4.12	10.08	26.55	6.45
B10–20	37.44	9.38	3.99	31.82	4.69	6.78	13.32	2.84
B10–30	31.06	9.56	3.25	26.40	6.21	4.25	11.95	1.93
B12–0	63.97	9.17	6.97	54.37	5.34	10.18	20.94	3.92
B12–10	62.59	11.74	5.33	53.20	6.71	7.92	18.69	2.78
B12–20	44.34	11.42	3.88	37.68	6.67	5.65	21.59	3.24
B12–30	38.68	12.11	3.19	32.87	6.73	4.89	21.61	3.21

*P_{max} is maximum load, P_y is load at 0.85 P_{max}, δ_{Pmax} is displacement at P_{max}, δ_y is displacement at 0.85 P_{max}, δ_u is ultimate displacement at 0.85 P_{max}, S_{Pmax} is stiffness at P_{max}, and S_y is stiffness at P_y.

capacity (P_{max}) by 5.8% and 2.2%, respectively. However, these decreases were at reasonable levels. The CP incorporation up to 10%, in other words the optimum ratio, increased the compressive and flexural strengths of concrete, since it acted as a filler material as well as having pozzolanic reactivity [60,61]. The reason for this issue is explained in the studies of the literature as follows. Ceramic combination in the mixtures is mainly responsible for the alteration in porosity of mortars, which in turn enhances the compressive strength. The highest compressive strength was achieved in the mixture with 10% (having 10% CP and 100% ceramic fine replacement of cement and sand). The strength increased in the mixture with 10% may be as a consequence of the filler action (contributed by CP which is higher than cement) and the pozzolanic action of the entire combination [62]. As stated by Jamil et al. [63] and Chindaprasirt and Rukzon [64], the filler action supports the strength enhancement in blended cement concrete, and it takes place while the substitute material is better than cement. Addition of more than 10% CP led to a decrease in the strength, because the hydraulic binder material was replaced with a non-hydraulic material at a high rate [65].

In addition, the contribution of CP up to 10% almost did not influence the ultimate displacement capacities of RCBs. Meanwhile, the initial stiffness of RCBs was not affected by the 10% CP contribution. However, these RCBs' yield stiffness (S_y) and stiffness under maximum force (S_{Pmax}) decreased by 20% and 80%, respectively, compared with the reference RCBs. The stiffness tended to decline depending on the amount of CP, and the obtained results are compatible with similar literature studies [66,67]. Because of all these reasons, CP can be utilized up to 10% with caution since it created a reasonable decrease in the strength and stiffness of RCBs. However, more than 10% CP reduced the RCBs' strength, ductility, and stiffness at high rates.

4.3. Energy dissipation

The total energy dissipation of RCBs can considerably affect the level of earthquake damage and associated deformations when these members provide sufficient ductility [68,69]. The shear failure resulted in very low energy dissipation capacity; therefore, it should be avoided [70–74]. Table 5 demonstrates the experimentally determined energy dissipation capacities of RCBs. B8–10, provided the maximum total energy dissipation of 2.2 kj during the test procedures. Test results of B12–0, B12–10, B10–10, B12–20, B10–20, B12–30, B10–30, and B8–30 were achieved as out of the limits concerning their ductility levels. It can also be seen from Table 5 that the ductility levels of B8–0 and B8–10 were acceptable . More than 10% CP decreased the ductility levels and energy dissipation results due to its overdose usage [75–77].

4.4. Theoretical calculation results and comparison with experimental results

In this study, the equivalent rectangular stress distribution method was proposed from ACI 318–19 [55], Hognestad [52], Park et al. [53], and Todeschini et al. [54]. The RCBs' maximum flexural capacities (P_{max}) were calculated using the concrete stress-strain models and summarized in Table 6. Table 6 also lists the so-called shear capacities (V_n) of RCBs calculated according to ACI 318–19 [55].

As mentioned in Table 6, although the theoretical shear capacities (V_n) of all RCBs were at least 32% higher than the experimental results, the experimental flexural strengths of some of RCBs were well below the theoretical flexural capacities calculated according to ACI 318–19 [55]. These RCBs are B8–30, B10–20, B10–30, B12–20, and B12–30. As stated in Section 4.1, except for B8–0 and B8–10, pure flexural failure did not occur as expected, and either shear or flexural shear failure occurred unexpectedly. This point indicates that the excess CP affected the shear capacity more negatively than the calculated one. Especially when more than 10% CP was used, RCBs performed well below the theoretical flexural capacity.

When the flexural capacities of CP blended RCBs were examined using different concrete models, it was seen that the flexural capacities of RCBs with low reinforcements ratio (B8 series) were very similar, but as the reinforcements ratio increased (B12 series), the differences among the concrete models became apparent. Nonetheless, these differences become even more owing to the decrease

Table 5
Energy dissipation capacities resulted from experimental tests.

Test Specimen	δ_{max} (mm)	E_{Pmax} (kj)	E_y (kj)	E_p (kj)	E_T (kj)	Failure Type	Ductility Level
B8–0	62.49	2.25	0.25	2.14	2.39	FT	Sufficient
B8–10	60.58	1.86	0.46	1.74	2.20	FT	Sufficient
B8–20	33.40	0.83	0.23	0.82	1.05	FS	Partially Sufficient
B8–30	40.35	0.34	0.11	0.73	0.85	S	Deficient
B10–0	27.15	1.26	0.07	1.24	1.31	FS	Partially Sufficient
B10–10	40.12	0.89	0.16	1.42	1.59	FS	Deficient
B10–20	33.29	0.29	0.11	0.68	0.78	S	Deficient
B10–30	19.88	0.22	0.13	0.29	0.42	S	Deficient
B12–0	28.94	0.80	0.22	1.31	1.53	S	Deficient
B12–10	29.06	0.65	0.47	0.91	1.39	S	Deficient
B12–20	27.77	0.58	0.19	0.81	1.00	S	Deficient
B12–30	27.96	0.43	0.16	0.71	0.87	S	Deficient

* δ_{max} is maximum displacement, E_{Pmax} is energy dissipation at P_{max}, E_y is energy dissipation at P_y, E_p is plastic energy dissipation (E_T-E_y), E_T is total energy dissipation, FT is flexural tension failure, FS is flexural shear failure, and S is shear failure (diagonal tension failure).

Table 6
Calculated flexural and shear capacities of RCBs.

Test Specimen	P_{max} (kN)					$P_{Calc.}/P_{Exp.}$				V_n (kN)				$V_n/V_{Exp.}$
	Exp.	ACI	Hog.	Tod.	Park.	ACI	Hog.	Tod.	Park.	Exp.	V_c	V_s	V_n	
B8–0	40.7	35.8	35.4	35.5	35.9	0.88	0.87	0.87	0.88	20.4	6.7	33.7	40.4	1.98
B8–10	40.6	35.6	35.2	35.3	35.7	0.88	0.87	0.87	0.88	20.3	6.5	32.7	39.2	1.93
B8–20	36.6	35.1	34.7	34.2	35.3	0.96	0.95	0.94	0.96	18.3	5.9	29.6	35.5	1.94
B8–30	29.5	33.7	33.7	29.9	34.8	1.14	1.14	1.01	1.18	14.8	4.7	24.0	28.7	1.95
B10–0	51.7	49.5	47.9	47.3	48.6	0.96	0.93	0.92	0.94	25.8	7.7	33.7	41.5	1.61
B10–10	48.8	49.1	47.5	46.3	48.3	1.01	0.97	0.95	0.99	24.4	7.5	32.7	40.2	1.65
B10–20	37.4	47.7	46.4	40.6	47.7	1.28	1.24	1.08	1.28	18.7	6.8	29.6	36.4	1.95
B10–30	31.1	40.6	40.5	31.1	46.2	1.31	1.31	1.00	1.49	15.5	5.5	24.0	29.5	1.90
B12–0	64.0	61.9	59.5	52.2	60.3	0.97	0.93	0.82	0.94	32.0	8.7	33.7	42.5	1.33
B12–10	62.6	59.9	57.5	49.7	59.5	0.96	0.92	0.79	0.95	31.3	8.5	32.7	41.2	1.32
B12–20	44.3	53.8	51.8	42.6	56.4	1.21	1.17	0.96	1.27	22.2	7.7	29.6	37.3	1.68
B12–30	38.7	42.9	41.8	32.0	49.0	1.11	1.08	0.83	1.27	19.3	6.2	24.0	30.2	1.56

*Calc. = Calculation, Exp. = Experiment, ACI = ACI 318–19 [55], Hog. = Hognestad [52], Tod. = Todeschini et al. [54], and Park. = Park et al. [53].

in the compressive strength of concrete. Especially in B10–30 and B12–30, differences of up to 49% and 52% occurred among the concrete models, respectively. In this respect, it could not be determined which concrete model was more accurate due to the shear failure. For this reason, it was observed that additional studies are needed to verify the concrete models to be used to calculate the flexural capacities of CP blended RCBs.

5. Conclusions

This study focused on the utilization and effects of CP on the flexural performance of RCBs. The following main conclusions can be drawn:

- As cement was replaced with CP, it was witnessed that there was a reduction in the compressive strength values. Furthermore, the splitting tensile strength tests revealed that the splitting tensile strength values commonly followed the similar trend as the compressive strengths. By inserting 10% CP by the weight of cement, the splitting tensile strength was only 13.8% lower than the reference specimen.
- As the CP replacement increased from 0% to 10%, 20%, and 30%, the load-carrying capacity decreased between 0.4% and 27.5% compared with B8-0. However, 5.5−39.8% and 2.15−39.5% reductions occurred in the load-carrying capacity compared with B10-0 and B12-0, respectively.
- CP generally decreased the maximum and ultimate loads at similar intervals. With the ϕ8 tension bar, CP can be utilized effectively compared with the other used reinforcements types.
- The CP incorporation up to 10%, or the optimum replacement ratio, increased the compressive and flexural strengths of concrete, as it acted as both a filler material and pozzolanic reactive material.
- The utilization of CP more than 10% negatively impacted the ductility and energy dissipation tests results due to its overdose.
- For B8-0, B8-10, and B10-0, initially, the specimens' stiffness degraded significantly, while their carrying capacity degraded slightly, and their energy dissipation capacity remained relatively high. This showed that this type of RCB is greatly suitable for engineering applications and is anticipated to reduce the amount of cement required.
- All the RCBs' theoretical shear capacities (V_n) approximated the experimental results between 32% and 98%. This issue signified that CP affected the shear capacity more negatively than the calculated one. Especially when more than 10% CP was used (B8-30, B10-20, B10-30, B12-20, and B12-30), RCBs performed well below the theoretical flexural capacity.
- The consumption of CP has a great influence both in terms of its ecological effect on the environment and performance of structures. It is believed that it will be helpful for future sustainable designs, particularly for structural engineers.
- Using this study, the important opportunity of consuming CP as a sustainable material can be purposed for environmentally friendly concrete and reinforced concrete elements.

Declaration of Competing Interest

The authors declare that they have no known competing financial interests or personal relationships that could have appeared to influence the work reported in this article.

Data Availability

Data will be made available on request.

Acknowledgement

The authors are thankful to the Deanship of Scientific Research at Najran University for funding this research work, under the Research Groups Funding program grant code (NU/RG/SERC/12/11).

References

[1] A.İ. Çelik, T. Ufuk, A. Bahrami, M. Karalar, M.A.O. Mydin, T. Alomayri, et al., Use of waste glass powder toward more sustainable geopolymer concrete, J. Mater. Res. Technol. (2023).
[2] Y.O. Özkılıç, A.İ. Çelik, T. Ufuk, M. Karalar, A. Deifalla, T. Alomayri, et al., The use of crushed recycled glass for alkali activated fly ash based geopolymer concrete and prediction of its capacity, J. Mater. Res. Technol. (2023).
[3] H. He, S. E, T. Wen, J. Yao, X. Wang, C. He, Y. Yu, Employing novel N-doped graphene quantum dots to improve chloride binding of cement, Constr. Build. Mater. 401 (2023), 132944, https://doi.org/10.1016/j.conbuildmat.2023.132944.
[4] S. Zhou, C. Lu, X. Zhu, F. Li, Preparation and characterization of high-strength geopolymer based on BH-1 lunar soil simulant with low alkali content, Engineering 7 (2021) 1631–1645.
[5] P.O. Awoyera, J.O. Akinmusuru, J.M. Ndambuki, Green concrete production with ceramic wastes and laterite, Constr. Build. Mater. 117 (2016) 29–36.
[6] A.M. Mhaya, G.F. Huseien, A.R.Z. Abidin, M. Ismail, Long-term mechanical and durable properties of waste tires rubber crumbs replaced GBFS modified concretes, Constr. Build. Mater. 256 (2020), 119505.
[7] B. Basaran, I. Kalkan, C. Aksoylu, Y.O. Özkılıç, M.M.S. Sabri, Effects of waste powder, fine and coarse marble aggregates on concrete compressive strength, Sustainability 14 (2022) 14388.
[8] C. Aksoylu, Y.O. Özkılıç, M. Hadzima-Nyarko, E. Işık, M.H. Arslan, Investigation on improvement in shear performance of reinforced-concrete beams produced with recycled steel wires from waste tires, Sustainability 14 (2022) 13360.
[9] M. Karalar, Y.O. Özkılıç, A.F. Deifalla, C. Aksoylu, M.H. Arslan, M. Ahmad, et al., Improvement in bending performance of reinforced concrete beams produced with waste lathe scraps, Sustainability 14 (2022) 12660.
[10] M. Karalar, Y.O. Özkılıç, C. Aksoylu, M.M.S. Sabri, A.N. Beskopylny, S.A. Stel'Makh, et al., Flexural behavior of reinforced concrete beams using waste marble powder towards application of sustainable concrete, Front Mater. 9 (2022) 1068791.
[11] R. Garg, R. Garg, N.O. Eddy, M.A. Khan, A.H. Khan, T. Alomayri, et al., Mechanical strength and durability analysis of mortars prepared with fly ash and nano-metakaolin, Case Stud. Constr. Mater. 18 (2023), e01796.
[12] C.R. Kaze, L.M. Beleuk à Moungam, J.V. Sontia Metekong, T.S. Alomayri, A. Naghizadeh, L. Tchadjie, Thermal behaviour, microstructural changes and mechanical properties of alkali-activated volcanic scoria-fired waste clay brick blends, Dev. Built Environ. 14 (2023), 100153.
[13] A. Raza, T. Alomayri, M. Berradia, Rapid repair of partially damaged GFRP-reinforced recycled aggregate concrete columns using FRP composites, Mech. Adv. Mater. Struct. 29 (2022) 6070–6086.
[14] L. Gautam, J. Kumar Jain, T. Alomayri, N. Meena, P. Kalla, Performance evaluation of self-compacting concrete comprising ceramic waste powder as fine aggregate, Mater. Today.: Proc. 61 (2022) 204–211.
[15] Y.O. Özkılıç, M. Karalar, C. Aksoylu, A.N. Beskopylny, S.A. Stel'makh, E.M. Shcherban, et al., Shear performance of reinforced expansive concrete beams utilizing aluminium waste, J. Mater. Res. Technol. 24 (2023) 5433–5448.
[16] E.M. Shcherban', S.A. Stel'makh, A.N. Beskopylny, L.R. Mailyan, B. Meskhi, A.A. Shilov, et al., Normal-weight concrete with improved stress–strain characteristics reinforced with dispersed coconut fibers, Appl. Sci. 12 (2022) 11734.
[17] A.N. Beskopylny, E.M. Shcherban', S.A. Stel'makh, B. Meskhi, A.A. Shilov, V. Varavka, et al., Composition component influence on concrete properties with the additive of rubber tree seed shells, Appl. Sci. 12 (2022) 11744.
[18] Y. Han, S. Shao, B. Fang, T. Shi, B. Zhang, X. Wang, et al., Chloride ion penetration resistance of matrix and interfacial transition zone of multi-walled carbon nanotube-reinforced concrete, J. Build. Eng. 72 (2023), 106587.
[19] M. Wang, X. Yang, W. Wang, Establishing a 3D aggregates database from X-ray CT scans of bulk concrete, Constr. Build. Mater. 315 (2022), 125740.
[20] W. Zhang, S. Kang, X. Liu, B. Lin, Y. Huang, Experimental study of a composite beam externally bonded with a carbon fiber-reinforced plastic plate, J. Build. Eng. 71 (2023), 106522.
[21] C. Liu, J. Cui, Z. Zhang, H. Liu, X. Huang, C. Zhang, The role of TBM asymmetric tail-grouting on surface settlement in coarse-grained soils of urban area: Field tests and FEA modelling, Tunn. Undergr. Space Technol. 111 (2021), 103857.
[22] M. Samadi, M.H. Baghban, Z. Kubba, I. Faridmehr, N.H. Abdul Shukor Lim, O. Benjeddou, et al., Flexural behavior of reinforced concrete beams under instantaneous loading: effects of recycled ceramic as cement and aggregates replacement, Buildings 12 (2022) 439.
[23] B.B. Jindal, T. Alomayri, A. Hasan, C.R. Kaze, Geopolymer concrete with metakaolin for sustainability: a comprehensive review on raw material's properties, synthesis, performance, and potential application, Environ. Sci. Pollut. Res. (2022) 1–26.
[24] P. Lehner, M. Horňáková, Effect of amount of fibre and damage level on service life of sfr recycled concrete in aggressive environment, Buildings 11 (2021) 489.
[25] H.A. Algaifi, M.I. Khan, S. Shahidan, G. Fares, Y.M. Abbas, G.F. Huseien, et al., Strength and acid resistance of ceramic-based self-compacting alkali-activated concrete: optimizing and predicting assessment, Materials 14 (2021) 6208.
[26] B. Başaran, C. Aksoylu, Y.O. Özkılıç, M. Karalar, A. Hakamy, Shear behaviour of reinforced concrete beams utilizing waste marble powder, *Structures* 54 (2023) 1090–1100.
[27] L. Sun, C. Wang, C. Zhang, Z. Yang, C. Li, P. Qiao, Experimental investigation on the bond performance of sea sand coral concrete with FRP bar reinforcement for marine environments, Adv. Struct. Eng. 26 (2023) 533–546.
[28] Y.-n Wang, Q. Wang, Y. Li, H. Wang, Y. Gao, Y. Sun, et al., Impact of incineration slag co-disposed with municipal solid waste on methane production and methanogens ecology in landfills, Bioresour. Technol. 377 (2023), 128978.
[29] S. Seara-Paz, B. González-Fonteboa, F. Martínez-Abella, D. Carro-López, Long-term flexural performance of reinforced concrete beams with recycled coarse aggregates, Constr. Build. Mater. 176 (2018) 593–607.
[30] B. Zhao, G. Wang, B. Wu, X. Kong, A study on mechanical properties and permeability of steam-cured mortar with iron-copper tailings, Case Stud. Constr. Mater. 383 (2023), 131372.
[31] Y.O. Özkılıç, B. Başaran, C. Aksoylu, M. Karalar, C.H. Martins, Mechanical behavior in terms of shear and bending performance of reinforced concrete beam using waste fire clay as replacement of aggregate, Case Stud. Constr. Mater. 18 (2023), e02104.
[32] H.M. Magbool, Utilisation of ceramic waste aggregate and its effect on eco-friendly concrete: a review, J. Build. Eng. 47 (2022), 103815.
[33] S.K. Das, S.M. Mustakim, A. Adesina, J. Mishra, T.S. Alomayri, H.S. Assaedi, et al., Fresh, strength and microstructure properties of geopolymer concrete incorporating lime and silica fume as replacement of fly ash, J. Build. Eng. 32 (2020), 101780.
[34] O. Zimbili, W. Salim, M. Ndambuki, A review on the usage of ceramic wastes in concrete production, Int. J. Civ. Environ. Struct. Constr. Archit. Eng. 8 (2014) 91–95.
[35] Q. Chang, L. Liu, M.U. Farooqi, B. Thomas, Y.O. Özkılıç, Data-driven based estimation of waste-derived ceramic concrete from experimental results with its environmental assessment, J. Mater. Res. Technol. 24 (2023) 6348–6368.
[36] H.M. Najm, S. Ahmad, The effect of metallic and non-metallic fiber on the mechanical properties of waste ceramic concrete, Innov. Infrastruct. Solut. 6 (2021) 1–15.
[37] M. Samadi, G.F. Huseien, H. Mohammadhosseini, H.S. Lee, N.H.A.S. Lim, M.M. Tahir, et al., Waste ceramic as low cost and eco-friendly materials in the production of sustainable mortars, J. Clean. Prod. 266 (2020), 121825.

[38] R. Senthamarai, P.D. Manoharan, Concrete with ceramic waste aggregate, Cem. Concr. Compos. 27 (2005) 910–913.
[39] B. Huang, Q. Dong, E.G. Burdette, Laboratory evaluation of incorporating waste ceramic materials into Portland cement and asphaltic concrete, Constr. Build. Mater. 23 (2009) 3451–3456.
[40] R. Senthamarai, P.D. Manoharan, D. Gobinath, Concrete made from ceramic industry waste: Durability properties, Constr. Build. Mater. 25 (2011) 2413–2419.
[41] G.F. Huseien, A.R.M. Sam, K.W. Shah, J. Mirza, M.M. Tahir, Evaluation of alkali-activated mortars containing high volume waste ceramic powder and fly ash replacing GBFS, Constr. Build. Mater. 210 (2019) 78–92.
[42] M. Samadi, M.W. Hussin, H.S. Lee, A.R.M. Sam, M.A. Ismail, N.H.A.S. Lim, et al., Properties of mortar containing ceramic powder waste as cement replacement, J. Teknol. (2015) 77.
[43] G.F. Huseien, A.R.M. Sam, J. Mirza, M.M. Tahir, M.A. Asaad, M. Ismail, et al., Waste ceramic powder incorporated alkali activated mortars exposed to elevated Temperatures: Performance evaluation, Constr. Build. Mater. 187 (2018) 307–317.
[44] Fernandes M., Sousa A., Dias A. Environmental impacts and emissions trading-ceramic industry: a case study. Coimbra: Technological centre of ceramics and glass, Portuguese association of ceramic industry (in Portuguese). 2004.
[45] Mukai T., Kikuchi M. Studies on utilization of recycled concrete for structural members (Part 1, Part 2). Summaries of technical papers of annual meeting, Architectural Institute of Japan1978. p. 85–6.
[46] T. Mukai, M. Kikuchi, Properties of reinforced concrete beams containing recycled aggregate Proc. Second Int Symp. demolition reuse Concr. Mason. 1988 670 679.
[47] F. Pacheco-Torgal, S. Jalali, Compressive strength and durability properties of ceramic wastes based concrete, Mater. Struct. 44 (2011) 155–167.
[48] E. Ikponmwosa, S. Ehikhuenmen, Flexural behavior of concrete beams containing ceramic waste as replacement of coarse aggregate, Ann. Fac. Eng. Hunedoara 16 (2018) 159–164.
[49] E. Fatima, A. Jhamb, R. Kumar, Ceramic dust as construction material in rigid pavement, Am. J. Civ. Eng. Archit. 1 (2013) 112–116.
[50] I. Guerra, I. Vivar, B. Llamas, A. Juan, J. Moran, Eco-efficient concretes: the effects of using recycled ceramic material from sanitary installations on the mechanical properties of concrete, Waste Manag. 29 (2009) 643–646.
[51] H. Koyuncu, Y. Guney, G. Yılmaz, S. Koyuncu, R. Bakis, Utilization of ceramic wastes in the construction sector Key Eng. Mater.: Trans. Tech. Publ. 2004 2509 2512.
[52] E. Hognestad, Study of combined bending and axial load in reinforced concrete members Univ. Ill. Eng. Exp. Station Bull. no 399 1951.
[53] R. Park, M.N. Priestley, W.D. Gill, Ductility of square-confined concrete columns, J. Struct. Div. 108 (1982) 929–950.
[54] C.E. Todeschini, A.C. Bianchini, C.E. Kesler, Behavior of concrete columns reinforced with high strength steels, J. Proc. (1964) 701–716.
[55] A. Committee Building code requirements for structural concrete and commentary (ACI 318-19) Am. Concr. Inst.: Farming Hills, MI, USA 2019 623.
[56] A. Heidari, D. Tavakoli, A study of the mechanical properties of ground ceramic powder concrete incorporating nano-SiO2 particles, Constr. Build. Mater. 38 (2013) 255–264.
[57] P. Kuan, Q. Hongxia, C. Kefan, Reliability analysis of freeze–thaw damage of recycled ceramic powder concrete, J. Mater. Civ. Eng. 32 (2020) 05020008.
[58] H. Naderpour, K. Nagai, Shear strength estimation of reinforced concrete beam–column sub-assemblages using multiple soft computing techniques Struct. Des. Tall Spec. Build. 29 2020 e1730.
[59] Türker K., Yavaş A., Birol T., Gültekin C. Evaluation of using ultra-high performance fiber reinforced concrete in I-section RC beam. 2021.
[60] M. Mohit, Y. Sharifi, Ceramic waste powder as alternative mortar-based cementitious material, Acids Mater. J. 116 (2019) 107–116.
[61] M. Mohit, Y. Sharifi, Thermal and microstructure properties of cement mortar containing ceramic waste powder as alternative cementitious materials, Constr. Build. Mater. 223 (2019) 643–656.
[62] P.O. Awoyera, A.R. Dawson, N.H. Thom, J.O. Akinmusuru, Suitability of mortars produced using laterite and ceramic wastes: Mechanical and microscale analysis, Constr. Build. Mater. 148 (2017) 195–203.
[63] M. Jamil, M.N.N. Khan, M.R. Karim, A. Kaish, M.F.M. Zain, Physical and chemical contributions of Rice Husk Ash on the properties of mortar, Constr. Build. Mater. 128 (2016) 185–198.
[64] P. Chindaprasirt, S. Rukzon, Strength and chloride resistance of the blended Portland cement mortar containing rice husk ash and ground river sand, Mater. Struct. 48 (2015) 3771–3777.
[65] A.S. El-Dieb, D.M. Kanaan, Ceramic waste powder an alternative cement replacement–Characterization and evaluation, Sustain. Mater. Technol. 17 (2018), e00063.
[66] R.J. Daniel, S. Sangeetha, Experimental study on concrete using waste ceramic as partial replacement of aggregate, Mater. Today.: Proc. 45 (2021) 6603–6608.
[67] Sharba A. Possibility of using waste glass powder and ceramic tile as an aggregate on the flexural behavior and strength properties. Proceedings of the 1st International Multi-Disciplinary Conference Theme: Sustainable Development and Smart Planning, IMDC-SDSP 2020, Cyperspace, 28–30 June 20202020.
[68] Yuan W., Tian-qi W., Li-min S., Wen X. Experimental investigation on seismic performance of rectangular-hollow double-column tall piers with energy dissipation beams. 工程力学. 2020;37:159–67.
[69] L.-H. Xu, G. Zhang, S.-J. Xiao, Z.-X. Li, Development and experimental verification of damage controllable energy dissipation beam to column connection, Eng. Struct. 199 (2019), 109660.
[70] H. Huang, M. Li, Y. Yuan, H. Bai, Theoretical analysis on the lateral drift of precast concrete frame with replaceable artificial controllable plastic hinges, J. Build. Eng. 62 (2022), 105386.
[71] H. Huang, M. Li, W. Zhang, Y. Yuan, Seismic behavior of a friction-type artificial plastic hinge for the precast beam–column connection, Arch. Civ. Mech. Eng. 22 (2022) 201.
[72] H. Huang, Y. Yuan, W. Zhang, M. Li, Seismic behavior of a replaceable artificial controllable plastic hinge for precast concrete beam-column joint, Eng. Struct. 245 (2021), 112848.
[73] H. Huang, M. Huang, W. Zhang, M. Guo, B. Liu, Progressive collapse of multistory 3D reinforced concrete frame structures after the loss of an edge column, Struct. Infrastruct. Eng. 18 (2022) 249–265.
[74] M. Guo, H. Huang, W. Zhang, C. Xue, M. Huang, Assessment of RC Frame Capacity Subjected to a Loss of Corner Column, J. Struct. Eng. 148 (2022) 04022122.
[75] I. Asiwaju-Bello, O. Olalusi, F. Olutoge, Effect of salt water on the compressive strength of ceramic powder concrete, Am. J. Eng. Res. 6 (2017) 158–163.
[76] H. Patel, N. Arora, S.R. Vaniya, Use of ceramic waste powder in cement concrete, Int. J. Innov. Res. Sci. Technol. 2 (2015) 91–97.
[77] Y.-h Cheng, F. Huang, R. Liu, J.-l Hou, G.-l Li, Test research on effects of waste ceramic polishing powder on the permeability resistance of concrete, Mater. Struct. 49 (2016) 729–738.
[78] M. Jin, Y. Ma, W. Li, J. Huang, Y. Yan, H. Zeng, J. Liu, Multi-scale investigation on composition-structure of C-(A)-S-H with different Al/Si ratios under attack of decalcification action, Cement and Concrete Research 172 (2023), 107251, https://doi.org/10.1016/j.cemconres.2023.107251.
[79] T. Shi, Y. Liu, Z. Hu, M. Cen, C. Zeng, J. Xu, Z. Zhao, Deformation performance and fracture toughness of carbon nanofiber-modified cement-based materials, ACI Materials Journal 119 (5) (2022) 119–128.
[80] D. Li, J. Nie, H. Wang, J. Yan, C. Hu, P. Shen, Damage location, quantification and characterization of steel-concrete composite beams using acoustic emission, Engineering Structures 283 (2023), 115866, https://doi.org/10.1016/j.engstruct.2023.115866.
[81] F. Zhou, H. Jiang, L. Huang, Y. Hu, Z. Xie, Z. Zeng, X. Zhou, Early Shrinkage Modeling of Complex Internally Confined Concrete Based on Capillary Tension Theory, Buildings 13 (9) (2023) 2201, https://doi.org/10.3390/buildings13092201.
[82] J. Cai, J. Pan, G. Li, M. Elchalakani, Behaviors of eccentrically loaded ECC-encased CFST columns after fire exposure, Engineering Structures 289 (2023), 116258, https://doi.org/10.1016/j.engstruct.2023.116258.